Development and Dosimetry of a Free-Space Type *in vitro* Exposure Apparatus for Millimeter-Waves

Sho Kurogi[#1], Hiroshi Saito[#], Takayuki Taguchi[#], Yukihisa Suzuki[#], Masao Taki[#2]

[#]*Department of Electrical and Electronic Engineering, Tokyo, Metropolitan University*

1-1, Minamiosawa, Hachioji, Tokyo, 192-0397, JAPAN

[1]kurogi@com.eei.metro-u.ac.jp

[2]masao@tmu.ac.jp

***Abstract*—We developed a free-space type *in vitro* exposure apparatus for 60 GHz millimetre-waves (MMWs). The SAR distribution in the medium was numerically obtained by the finite-difference time-domain (FDTD) method. Temperature distributions were estimated by numerical calculations of the equation of heat conduction. The numerical results were also investigated experimentally by using two different methods of temperature measurement. Temperature elevation was measured by fluoroptic thermoprobes. Temperature distribution was measured by micro-encapsulated thermo-chromic liquid crystal (MTLC). It is found that MTLC has advantages over fluoroptic probes owing to the very high spatial resolution and quick temporal response which provide useful means for MMW dosimetry.**

Key words: millimeter-waves, SAR, FDTD, *in vitro*, exposure apparatus, thermal analysis, MTLC

I. Introduction

The use of millimeter-waves (MMWs) is expected to increase various applications including short-range communications, radar systems and sensor networks. Human exposure to MMWs will be increasing in daily lives. Possible health risks should be carefully examined.

The exposure guidelines of electromagnetic fields [1] in the MMW region have been mainly derived from the extrapolation of the data obtained in microwaves and infrared optical radiations. It is necessary to investigate biological effects of MMWs through experiments directly [2 - 4].

The purpose of this study is the development and dosimetry of an exposure apparatus for *in vitro* experiments in MMW region. The penetration depth of MMWs is very small (less than 1 mm) in aqueous solutions such as culture medium. The spatial gradient of specific absorption rate (SAR) is very large in the medium, resulting in the steep temperature gradient. Some new approaches are necessary for dosimetry and thermal measurement for MMWs.

We developed a free-space type *in vitro* exposure apparatus for 60 GHz MMWs. The SAR distribution in the medium was numerically obtained by the finite-difference time-domain (FDTD) method. Temperature distributions were estimated by numerical calculations of the equation of heat conduction. The numerical results were also investigated experimentally by using two different methods of temperature measurement. Temperature elevation was measured by fluoroptic thermoprobes. Temperature distribution was measured by micro-encapsulated thermo-chromic liquid crystal (MTLC). It is found that MTLC has advantages over fluoroptic probes owing to the very high spatial resolution and quick temporal response which provide useful means for MMW dosimetry.

II. Exposure Apparatus for Cells

The exposure apparatus used in this study is shown in Fig. 1. This exposure apparatus employs a horn antenna as a basic structure. A culture dish is placed on the aperture of a horn antenna to achieve a sufficient exposure area. A Gunn oscillator (Quinstar Technology, INC. QBY-603400) generates MMW of 60 GHz band. The output power is applied to an IMPATT amplifier, and the maximum output power is approximately 2 W.

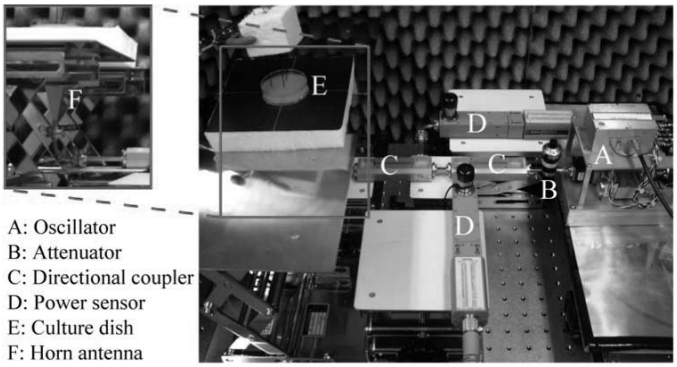

Fig. 1 The free-space type exposure apparatus using horn antenna

III. Electromagnetic Field Analysis

A. Model for FDTD calculation

The SAR distribution in the culture medium was calculated using FDTD method [5]. SEMCAD X (Schmid & Parther Engineering AG.) was used for the calculation.

The model of the apparatus for FDTD calculation is shown in Fig. 2. We employed variable grid from 0.1mm to 0.2 mm in the culture medium. The source generates TE_{10} waves at 60 GHz toward the positive direction of the z-axis, and they are expanded by the horn antenna. The total power fed from the source to the aperture of the horn antenna was normalized to 1 W. Uniaxial perfectly matched layers (UPML) [5] was applied

to the boundary condition. The thickness of the polystyrene culture dish was 1.0 mm and its internal diameter was 52mm. The thickness of the culture medium was determined 3 mm. The SAR of the culture medium was calculated by using the following equation:

$$SAR = \frac{\sigma E^2}{\rho}, \quad (1)$$

where E is the effective value of electric field, σ is the conductivity and ρ is the density. The electrical constants of the culture dish [6] and the medium [7] are shown in Table 1.

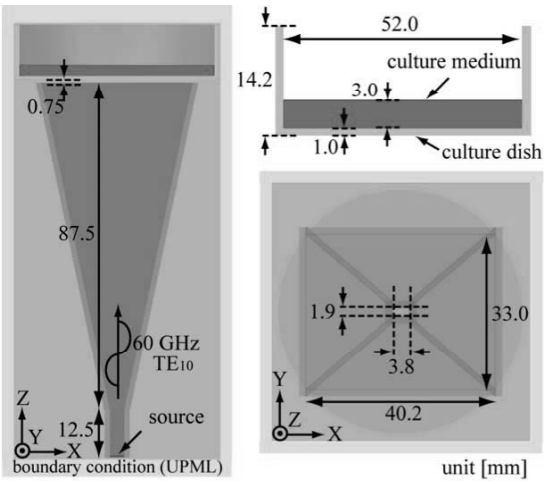

Fig. 2 Model of the exposure apparatus for electromagnetic field calculation

TABLE 1

ELECTRICAL CONSTANS USED IN THE FDTD CALCULATION

	air	culture medium [6]	culture dish [7]
ε_r	1.0	12.1	2.6
σ [S/m]	0.0	69.4	0.0

B. Results of FDTD calculation

We assume the bottom of the culture medium as the location of cells as adherent cells are to be used for the experiments. The calculated SAR distribution is shown in Figs. 3 and 4, for the X-Y plane in the bottom layer of the medium and the Y-Z plane along the cross section D, respectively. The results of SAR distribution are shown in Table 2. The maximum SAR was appeared on the bottom of the medium, and average SAR in the bottom layer was 1.57×10^3 W/kg per 1 W output power from the horn antenna.

TABLE 2

THE RESULTS OF SAR DISTRIBUTION

	on the bottom	total medium
number of voxels	52116	1355020
maximum SAR [W/kg]	7.94×10^3	7.94×10^3
average SAR [W/kg]	1.57×10^3	113

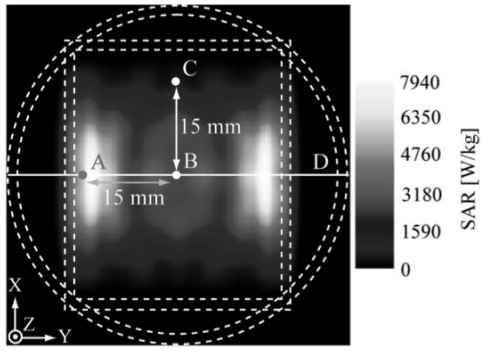

Fig. 3 SAR distribution in the X-Y plane on the bottom layer of the medium

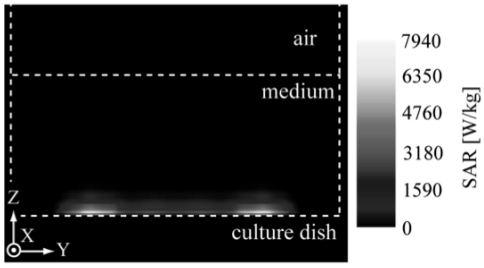

Fig. 4 SAR distribution in the Y-Z plane along the cross section D

IV. THERMAL ANALYSIS AND MEASUREMENT

A. Equation of heat conduction

We investigate the thermal fields of the medium in the dish by using the SAR distributions obtained in the previous section. When heat convection is neglected, the thermal fields are described by the following equations:

$$\rho c \frac{\partial T}{\partial t} = -\nabla \cdot \vec{q} + \rho SAR, \quad (2)$$

$$\vec{q} = -\nabla T, \quad (3)$$

where T is the temperature, $\vec{q}$ is the heat flux, ρ is the density, c is the specific heat and k is the heat conductivity.

Additionally, heat flux $\vec{q}$ in the direction of the normal vector on the boundary between the object (medium and culture dish) and the air is determined by the boundary condition:

$$\vec{q} \cdot \vec{n} = h(T - T_{air}), \quad (4)$$

where h is heat transfer coefficient on the boundary, and T_{air} is air temperature far from the boundary. The temperature distribution in the object was calculated by these equations with an explicit finite difference method.

The model of the object with curved surfaces has staircases on the boundary when orthogonal grid is used. The heat transfer coefficient h was modified taking the staircase effects into account.

B. Calculation conditions

Table 3 shows the values of the heat transfer coefficient, the density and the specific heat of each material [8]. Values of medium were assumed as those of water.

TABLE 3

CONSTANTS OF EACH MATERIAL USED IN THE CALCULATION [8]

	ρ [kg/m^3]	c [J/K·kg]	k [W/m·K]
medium	1.0×10^3	4.2×10^3	6.0×10^{-1}
dish	1.1×10^3	1.3×10^3	8.0×10^{-2}

The followings are calculation conditions.

· Time step Δt : 0.02 s

· Grid size Δx, Δy : 0.2 mm, Δz : 0.1 mm

· Heat transfer coefficient h on the boundary : 30 W/m^2·K

· Initial temperature : 22 ^{o}C

· Air temperature far from the boundary T_{air} : 22 ^{o}C

· Output power from the horn antenna: 2 W

For natural flow gas convection, a typical value of heat transfer coefficient is reported 5-30 W/m^2·K [9], so we assumed heat transfer coefficient h = 30 W/m^2·K. Grid sizes are almost equal to those of electromagnetic analysis in the object.

C Results of thermal analysis

Temperature distributions of the medium were calculated on the same calculation conditions. Figure 5 shows the temperature distribution in the X-Y plane in the bottom layer of the medium at 8 second from the onset of the exposure. Figure 6 shows the temperature distribution in the Y-Z plane along the cross section D defined in Fig. 3 at 18 second.

Temperature distributions shown in Figs. 5 and 6 were consistent with the distribution of SAR in Figs. 3 and 4. Temperature of the medium elevated approximately 5 degrees at the maximum SAR point. The steep temperature gradient was found in the medium.

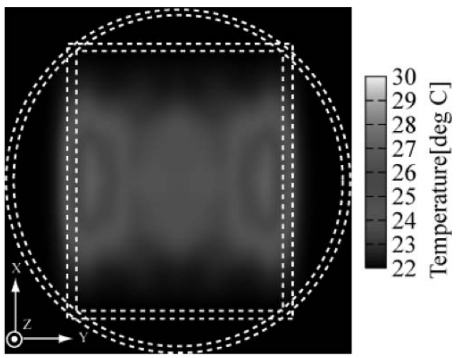

Fig. 5 Temperature distribution in the X-Y plane on the bottom layer of the object at 8 second by thermal analysis

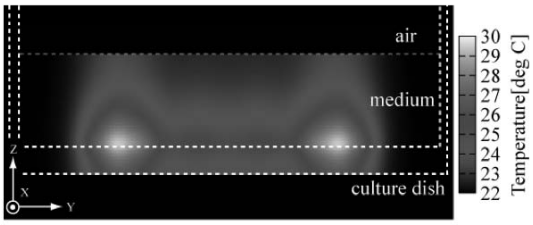

Fig. 6 Temperature distribution in the Y-Z plane along the cross section D (see Fig. 3) at 18 second by thermal analysis

D. Temperature elevation measured with fluoroptic thermoprobe

The result of numerical calculation was experimentally confirmed. The SAR on the bottom of the medium was estimated from measured temperature elevation by using the following equation [10]:

$$SAR \approx c\frac{\Delta T}{\Delta t}, \quad (5)$$

where c is the specific heat, ΔT is the temperature elevation, and Δt is the exposure time duration. Δt must be short enough for heat conduction to be ignored.

The measurement was made with an output power of 2 W. A fluoroptic thermoprobe (Anritsu Meter Co., Ltd. FL-2000) was used to measure the temperature of the medium during exposure. The measurement points were three points shown in Fig. 3. Agar was mixed into the medium prevent the convection. The measurement was performed five times, and the data were averaged. The room temperature was kept 22 ℃.

E. Measured results with fluoroptic thermoprobes

Figure 7 shows the comparison between the numerical calculation and the measurement with thermoprobe placed on the bottom the medium. While the calculated temperature on the bottom elevated immediately, the measured temperature elevation delayed for several seconds.

Table 2 shows estimated SARs form measurement. SAR was estimated from the temperature elevation during 10 to 20 second where the steepest temperature elevation occurred. The average SAR on the bottom of the medium was not reproduced, however. The discrepancy should be attributed to the insufficient spatial resolution and large heat capacity of the fluoroptic element of thermoprobe.

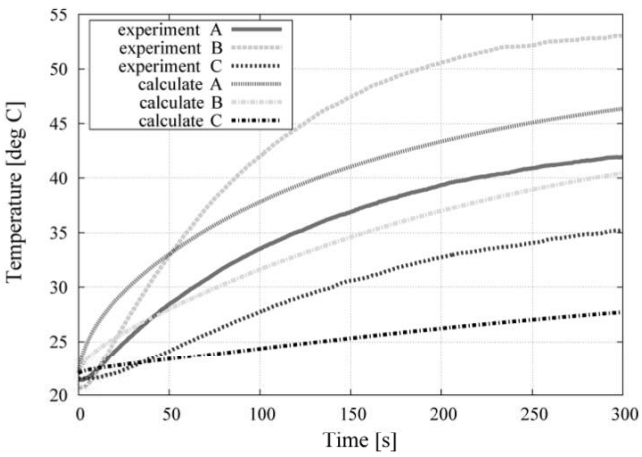

Fig. 7 Comparison of temperature elevation on the bottom of the medium during exposure between the numerical calculation and the measurement

TABLE 2

ESTIMATED SAR FROM TEMPERATURE ELEVATION MEASUREMENT

	A	B	C
SAR [w/kg]	773	1.24×10^3	168

V. Temperature distribution measured with MTLC[11]

A. MTLC method

Micro-encapsulated thermo-chromic liquid crystal (MTLC) was employed as the micro temperature probe. MTLC has a spatially high resolution and a high sensitivity to changes in temperature. The diameter of MTLC is between 20 and 30 μm. MTLC was homogeneously suspended in transparent material to measure temperature distribution. The slit light was projected into the material. Temperature distribution was visualized within the cross section illuminated by the slit light. We observe temperature distribution with rainbow color visualized from red to blue.

We used carrageenan gel [11], because carrageenan gel has higher transparency than agar gel used in the previous section. The mixture ratio of MTLC is 0.1 wt% and 0.02 wt% when the thickness of carrageenan gel was 1 mm and 3 mm, respectively. MTLC was toned depending on temperature from 25 ºC to 30 ºC in this study. MTLC changes its color from red, yellow, green, to blue according to temperature elevation.

B. Measured results with MTLC

Figure 8 (a) shows the experimental setup for the temperature distribution measurement with MTLC method. The carrageenan gel was illuminated by the slit light of 1 mm in thickness from X direction. Visualized temperature distribution was observed by a CCD camera as shown in Fig. 8 (a). Figure 8 (b) shows the visualized temperature distribution by MTLC after 8 second from the onset of the MMW exposure. It was found that the temperature profile obtained by MTLC method was similar to that calculated by the thermal analysis shown in Fig. 5.

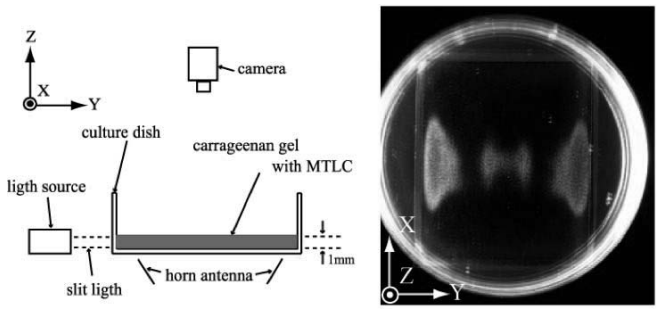

(a) (b)

Fig. 8 (a) Setup of temperature distribution measurement with MTLC. (b) Temperature distribution visualized by MTLC in the X-Y plane at the bottom of culture dish

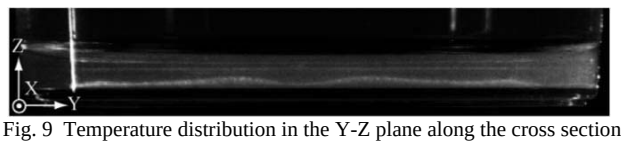

Fig. 9 Temperature distribution in the Y-Z plane along the cross section D

Figure 9 shows the temperature distribution in the Y-Z plane along the cross section D defined by Fig. 3. The thickness of the carrageenan gel was 3 mm. This result was obtained after 18 second from the onset of the MMW exposure. The temperature distribution shown in Fig. 9 is also similar to that calculated by thermal analysis shown in Fig. 6.

These results indicate that MTLC method has advantages over the measurement with fluoroptic thermoprobe. MMW exposure causes highly localized energy absorption and generates steep temperature gradient within several millimeter areas. MLTC can visualize those characteristics of changes in *in-situ* temperature distribution.

VI. Conclusion

We developed a free-space type *in vitro* exposure apparatus for MMWs. The SAR distribution and temperature distributions in the medium were obtained by numerical calculations. The dosimetry was performed by temperature measurement with fluoroptic thermoprobes and MTLC. As results, we found that it was impossible for fluoroptic thermoprobe to measure the local temperature. MTLC could measure owing to the very high spatial resolution and quick temporal response. MTLC provides useful means for MMW dosimetry.

Acknowledgments

This work was supported in part by the Committee to Promote Research on the Possible Biological Effects of Electromagnetic Fields, Ministry of Internal Affairs and Communications.

References

[1] International Commission on Non-Ionizing Radiation Protection, "Guidelines for limiting exposure to time-varying electric, magnetic, and electromagnetic fields (up to 300 GHz)" Health Phys., vol. 74, no.4, pp. 494-522, 1998.

[2] A. G. Pakhomov *et al.*, "Current State and Implications of Research on Biological Effects of Millimeter Waves: A Review of the Literature" Bioelectromagnetics., vol. 19, no. 7, pp. 393-413, Jan, 1998.

[3] I. Szabo *et al.*, "Millimeter Wave Induced Reversible Externalization of Phosphatidylserine Molecules in Cells Exposed in Vitro" Bioelectromagnetics., vol. 27, no. 3, pp. 233-244, Jan, 2006.

[4] J. Zhao, and Z. Wei, "Numerical Modeling and Dosimetry of the 35 mm Petri Dish Under 46 GHz Millimeter Wave Exposure" Bioelectromagnetics., vol. 26, no. 6, pp. 481-488, Jan, 2005.

[5] A. Taflove, and S. C. Hagness, "Computational electromagnetics the finite difference time domain method" Artech House INC, Norwood, 2005.

[6] T. Sonoda *et al.*, "Electromagnetic and Thermal Dosimetry of a Cylindrical Waveguide-Type *in vitro* Exposure Apparatus" IEICE TRANS. COMMUN., vol. E88-B, no. 8, pp. 3287-3293, August, 2005.

[7] H. Saito *et al.*, "Measurement of Complex Permittivity for Biological Cells by Waveguide Penetration Method" EMC'09., Kyoto, Japan, July, 2009.

[8] National Astronomical Observatory of Japan ed., "The chronological table of science" Maruzen, Tokyo, 2001.

[9] A. Nakayama, F.Kuwahara, and K. Kokuryou, "Netsu Ryutai Rikigaku" Kyoritsu-Shuppan, Tokyo, 2002.

[10] M. A. Stuchly and S. S. Stuchly, "Experimental radiowave and microwave dosimetry" in CRC Handbook of Biological Effects of Electromagnetic Fields second edition, eds. C. Polk and E. Postow, pp. 314-322, CRC press, New York, 1995.

[11] Y. Suzuki *et al.*, "Imaging the 3D Temperature Distributions Caused by Exposure of Dielectric Phantoms to High-Frequency Electromagnetic Fields" IEEE Trans. on Electr. Insul., vol. 13, no. 4, pp. 744-750, August, 2006.